



DØnote 4754-CONF

## High $P_T$ Cross Section for $\mu$ -Tagged Jets in $p\bar{p}$ Collisions at $\sqrt{s} = 1960$ GeV

The DØ Collaboration  
URL <http://www-d0.fnal.gov>  
(Dated: March 9, 2005)

The DØ Collaboration presents the inclusive jet cross section for  $\mu$ -tagged jets, using  $294 \text{ pb}^{-1}$  of integrated luminosity. Jets are defined using an  $(y, \phi)$  algorithm, with  $\Delta R < 0.5$ . Jets are considered  $\mu$ -tagged if they have a muon in the final jet cone. The analysis is restricted to  $|y_{\text{jet}}| < 0.5$ . An unsmearing procedure extracts the cross section at the particle level. The final result is then corrected to present the cross section for  $\mu$ -tagged jets exclusively from heavy flavor. This cross section is compared both to Pythia and a simple NLO theory.

*Preliminary Results for Winter 2005 Conferences*

## I. INTRODUCTION

One of the unsolved questions in the Standard Model is the question of particle generations. Why is it that there exist two carbon copies of the particles that make up everything we see? While there exists no answer to this question, one possibility is that quarks and leptons are composed of even smaller particles. The second and third generations could then simply be excited states of the ground state represented by the first generation.

If this hypothesis were true, then perhaps the third generation would show the largest deviation from point-like, Standard Model behavior. Towards this end, we are investigating the process  $X \rightarrow b\bar{b}$ , where  $X$  reflects possible new physics. As an interim analysis, we present here the inclusive cross section of jets with a collinear muon as a function of jet transverse momentum. Jets with collinear muons are expected to have an enhanced heavy flavor content. While our primary interest concerns jets containing both a muon and a  $b$ -quark-containing hadron (i.e. an inclusive  $b$  sample), separating the  $b$  and  $c$  quark content requires a separating variable, usually determined from Monte Carlo input. In order to present an experimentally well-defined quantity, we do not separate out a purely  $b$ -jet content, but rather present the purely inclusive  $\mu$ -tagged jet cross section, with the restriction that the jet also contain heavy flavor.

This analysis was performed at the Fermilab Tevatron, using the DØ detector. The DØ detector [1] consists of central tracking systems, composed of silicon and scintillating fiber sub-detectors, surrounded by a compensating calorimeter. Outside the calorimeter is a muon detection system, consisting of proportional drift tubes and scintillator. The central tracking volume is filled with a 2 Tesla magnetic field, oriented along the beam direction. The muon system includes a magnetized toroid. The integrated luminosity for this analysis is  $294 \text{ pb}^{-1}$ .

While the details of the analysis will be described below, a summary of the analysis is as follows. Jets are determined using a standard  $(y, \phi)$  cone algorithm, with  $R = 0.5$ . If a jet has a reconstructed muon within the cone radius (although the muon is *not* used in jet-finding), the jet is considered to be muon tagged. This analysis presents the  $\mu$ -tagged cross section for jets with  $|y| < 0.5$ . The presented result is restricted to only jets with muons from heavy flavor decay (i.e. muons for whom their creation vertex was within a few centimeters of the primary vertex). The cross section is corrected to remove those muons from pion and kaon decay. An unsmearing algorithm is applied, which results in a particle-level measurement of the  $\mu$ -tagged jet cross section, where the parent of the muon was a hadron containing heavy flavor ( $b$  or  $c$  quarks).

## II. EVENT SELECTION

The DØ QCD trigger proceeds through multiple stages: at Level 1, it requires a number of projective calorimeter towers above a  $P_T$  threshold, at Level 2 jets are formed using a simple cone algorithm and a low  $P_T$  threshold and finally at Level 3, higher  $P_T$  thresholds are imposed. Events were recorded using 4 triggers, with Level 3  $P_T$  trigger thresholds of 25, 45, 65 and 95 GeV. For this data set, the highest  $P_T$  trigger was unrescaled, while the lower threshold triggers had a luminosity-dependent prescale applied. The data set started with slightly more than 40M events. The run number for each event was compared to a database that recorded “good” runs. A run was considered good if there were no known problems with the silicon vertex system, central fiber tracker, calorimeter or muon system. In addition, the missing  $E_T$  and jet quality groups must report no problems with the run.

A preliminary skim was performed on the data to reduce the event count. Events were retained only if at least one of the two leading jets has a reconstructed muon within a  $\Delta R$  of 0.5 of the jet axis. After these cuts, we are left with 405,671 events. In order to further reduce the data set, a secondary skim was made. In this skim, the event is required to have a  $\mu$ -tagged jet with a central rapidity ( $|y| < 0.5$ ). Finally, for each event a loose  $P_T$  threshold was imposed on the  $\mu$ -tagged jet, appropriate for the trigger that fired the jet. The threshold chosen was such that the trigger was 90% efficient, leaving 18,328 events. This threshold was set on the  $P_T$  of the jet in question after full jet energy scale (more on that below) was applied. In the final stages of the analysis, trigger-specific thresholds were imposed, requiring the trigger be 100% efficient. We are left with 4,460 jets in the final analysis.

### A. Jets

Jets are defined using an iterative seed-based cone algorithm (including mid-points) with a radius in  $(y, \phi)$  space of 0.5 (where  $y = \frac{1}{2} \ln[(E + p_z)/(E - p_z)]$  is the rapidity and  $\phi$  is the azimuthal angle) [2]. The origin of the jets is taken to be the primary vertex, as reconstructed using tracks. Primary vertices are found using a Kalman filter method. Of all of the reconstructed primary vertices, the one that a maximum likelihood method states is *least* likely to be a minimum bias vertex is chosen.

## B. Muons

Muons in  $D\bar{O}$  are reconstructed using both the outer muon detector and the central tracker. The outer muon detector is located outside the calorimeter and consists of two parts, one of which is just outside the calorimeter (the A layer.) The A layer is followed by 1.09 meters of steel at normal incidence, outside of which are located the B and C layers. Each layer of the muon system consists of both scintillator and drift tubes. Because of the need to support the entire detector, there are no B and C layers on the bottom of the detector.

Because of the non-uniform detector placement, a reconstructed muon is defined differently in various parts of the detector [3]. The details of this variation are not critical, except to note that such a muon (denoted MEDIUM in the reference) on the bottom of the detector, by necessity, cannot require hits in the B and C layers of the detector. This is in contrast to the other regions in the detector, in which a signal in the BC layers is required. Because we are using muons *inside* jets, there exists the possibility that hadronic energy punch-through from the calorimeter will deposit energy in the A layer of the muon system. In conjunction with the track-rich environment of the core of a jet, one can reconstruct fake muons in this case. Studies of the  $\phi$  distribution of muons have shown that there exists an excess of  $\mu$ -tagged jets on the bottom of the calorimeter, which is taken as evidence for this punch-through. Thus in this analysis, we require a standard  $D\bar{O}$  MEDIUM muon, along with the requirement that there be at least one hit in the BC scintillator. This cut has a minimal effect for most solid angle, but forbid  $\mu$ -tagged jets from the bottom of the detector. Additional cuts include the requirement that the global fit of the muon candidate (using both the central track and muon system information) have a fit  $\chi^2 < 100$  and further the difference between the  $P_T$  of the corresponding central track and the global fit to the muon be less than 15 GeV. Neither of these cuts remove very many muon candidates, but they do preferentially remove poorly reconstructed muons.

## C. $\mu$ -Tagged Jet Energy Scale

Without further corrections, jets returned by the standard  $D\bar{O}$  reconstruction program do not have the correct momenta. Towards this end,  $D\bar{O}$  corrects jets back to the particle level [4] using a jet energy scale (JES) algorithm. This analysis uses the standard JES code, with a notable addition. Because the correction for jets with muons was determined primarily using Monte Carlo methods, we performed a cross-check. A subset of events was chosen with the following stringent criteria. The events were required to have two central ( $|y| < 0.5$ ) jets, with angular separation  $\Delta\phi > 2.84$ , one jet tagged with a muon and one not tagged with a muon. Finally, the number of jets both prior and after the jet quality cuts was required to be exactly two.

An asymmetry variable was defined:

$$A = 2 \frac{P_T(\mu) - P_T(\text{no } \mu)}{P_T(\mu) + P_T(\text{no } \mu)}. \quad (1)$$

This variable was plotted as a function of the average of the two jet's  $P_T = (P_T(\mu) + P_T(\text{no } \mu))/2$ . It was determined that, on average, the transverse momentum of the  $\mu$ -tagged jet was 3.8% higher than the corresponding non-muon-tagged jet. This factor was independent of average jet  $P_T$ , within the statistics available. Thus the  $P_T$  of each  $\mu$ -tagged jet was reduced by a factor of 1.038.

## D. $\mu$ -Tagged Jet Energy Resolution

Because a  $\mu$ -tagged jet also contains a collinear neutrino, its  $P_T$  resolution is degraded as compared to hadron-only jets. To determine the jet resolution, a plot very similar to that used for the JES correction was created, except the order of the jets was randomly assigned for the determination of the asymmetry variable of eq 1 (e.g. instead of  $P_T(\mu) - P_T(\text{no } \mu)$  always being the correct order,  $P_T(\text{no } \mu) - P_T(\mu)$  occurred with equal probability.) The RMS of this distribution was determined in bins of average jet  $P_T$  and taken as the combined resolution, including both the  $\mu$ -tagged and hadronic only jets.

Figure 1a shows the jet  $P_T$  difference RMS as a function of average jet  $P_T$ , with a fit overlay. The fit quality is such that  $\chi^2/\text{dof} = 10.8/12$ . Figure 1b shows the combined resolution for both jets, along with the independently-determined hadronic jet resolution and the extracted  $\mu$ -tagged jet resolution. In order to extract the final resolution, first the distribution of jet  $P_T$  RMS as a function of average jet  $P_T$  is fit to the equation:

$$\left(\frac{\sigma_{\text{measured}}}{P_{t, \text{measured}}}\right)^2 = \frac{N^2}{P_T^2} + \frac{S^2}{P_T} + C^2. \quad (2)$$

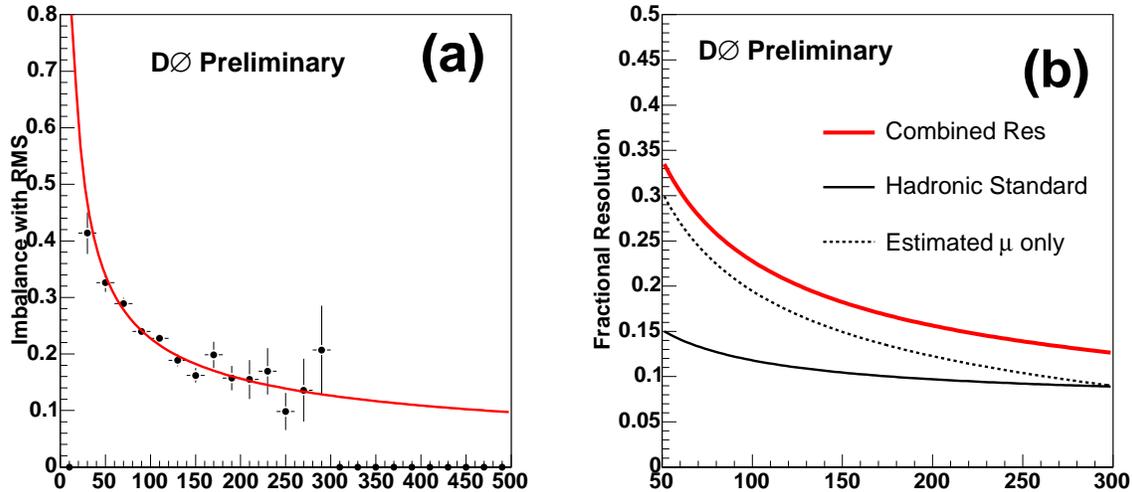


FIG. 1: (a) The RMS of the order-randomized asymmetry variable (i.e. the combined resolution  $P_T$  resolution of  $\mu$ -tagged and hadron-only jets. (b) Overlay of combined, hadron-only and extracted  $\mu$ -tagged resolution.

This will give the combined resolution of both jets. To extract the necessary  $\mu$ -tagged-only resolution, the hadronic-only resolution (determined separately by the DØ JES group [4]) must be removed. The behavior of the hadronic-only resolution is also parametrized as described in equation 2. The desired resolution is then extracted using:

$$\left(\frac{\sigma_{\mu \text{ jet}}}{P_{t, \mu \text{ jet}}}\right)^2 = \left(\frac{\sigma_{\text{measured}}}{P_{t, \text{measured}}}\right)^2 - \left(\frac{\sigma_{\text{no } \mu \text{ jet}}}{P_{t, \text{no } \mu \text{ jet}}}\right)^2 \quad (3)$$

Thus we have determined the resolution for  $\mu$ -tagged jets, with  $\mu$ -tagged-only parameters:  $N = 7.68 \pm 4.07$ ,  $S = 1.92 \pm 0.13$  and  $C = 0.00 \pm 0.08$ . The standard parabolic errors reported here neglect inter-parameter correlations.

### E. Efficiencies

The DØ detector records events with specific efficiencies for which we need to correct prior to final detector resolution unsmearing. The number of events in each bin of  $P_T$  can be given by the following equation.

$$N = \frac{\epsilon_T \epsilon_{PV} \epsilon_j \epsilon_\mu}{\mathcal{P}} \sigma_\mu \mathcal{L} \Delta P_T \quad (4)$$

where  $\epsilon_T$ ,  $\epsilon_{PV}$ ,  $\epsilon_j$  and  $\epsilon_\mu$  are the trigger, primary vertex, jet quality cut and muon-finding efficiencies respectively.  $\sigma_\mu$  is the cross section we want, while  $\mathcal{L}$  is the luminosity and  $\mathcal{P}$  is the purity.

The trigger efficiency  $\epsilon_T$  is 100% by construction. The jet quality cuts remove approximately 2% of the good jets, with an uncertainty determined by the details of how one projects the “good” distributions into the the cut regions. Thus  $\epsilon_j$  is set to  $99 \pm 1\%$ . The probability in a good jet event to reconstruct a primary vertex within 50 cm of the center of the detector is  $84 \pm 1\%$ .

The most uncertain of the efficiencies is that to reconstruct a muon. Because of the need to avoid the bottom of the DØ detector, we require the muon to be in the top of the detector, which imposes a 50% geometrical efficiency. In addition, the probability of reconstructing a muon is 84%. Finally, this analysis imposes an additional cut, requiring at least one hit in the scintillator of the B and C muon layers, which results in an additional 90% efficiency. Combining these three efficiencies gives a final muon-finding efficiency, to which is assigned a generous 10% error. Thus the muon-finding efficiency is  $37 \pm 3.7\%$

Assuming that the efficiencies are independent, we can combine them to give a final event efficiency of  $31 \pm 4\%$

## F. Unsmearing to Particle Level

Because of the finite resolution of the DØ detector, events in which the jet has a “true”  $P_T$  will be reconstructed to an observed  $P_T$  which is different than the truth. One must correct this smearing to extract a final result. In general, the observed distribution can be written  $F(P_T)$ , while the particle-level truth spectrum can be denoted  $f(P'_T)$ . The smearing function  $G(P'_T - P_T, P'_T)$  is usually taken to be a gaussian with mean 0 and RMS as specified in section II D. The observed spectrum can then be written as:

$$F(P_T) = \int_0^{\frac{\sqrt{s}}{2}} dP'_T \cdot f(P'_T) \cdot G(P'_T - P_T, P'_T) \quad (5)$$

One may then take various ansatzes for  $f(P'_T)$ , smear them according to the measured jet resolution and fit to the observed distribution. For this analysis, we used two ansatzes; they are:

$$f(P_T) = \sum_{j=1}^2 e^{N_j - \frac{P_T}{k_j}} \quad (6)$$

and

$$f(P_T) = N \cdot P_T^{-\alpha} \cdot e^{-\frac{P_T}{\beta}} \cdot \left(1 - \frac{2 \cdot P_T}{\sqrt{s}}\right)^\gamma \quad (7)$$

(where the last term specifically imposes a reduction in cross section at the kinematic limit and, for this analysis, the assignment  $\gamma = 0$  is imposed, as the  $P_T$  range presented here does not adequately constrain  $\gamma$ ).

The final comparison between the smeared function and the data is done by a simple  $\chi^2$  fit between the two, integrating the ansatz function over all  $P_T$  and the smeared function over each bin.

$$\chi^2 = \sum_{i=0}^{18} \frac{1}{\Delta y_i^2} \left( y_i - \frac{\int_{x_{1,i}}^{x_{2,i}} \int_0^{\sqrt{s}/2} f(P_T) \frac{1}{\sqrt{2\pi\sigma(P_T)}} e^{-\frac{(P_T - P_{T,m})^2}{2\sigma^2}} dP_T dP_{T,m}}{x_{2,i} - x_{1,i}} \right)^2 \quad (8)$$

where  $y_i$  and  $\Delta y_i$  are the observed efficiency-corrected data and error respectively. The data was separated into 18 bins and the RMS of the resolution function is  $P_T$  dependent. To do a final correction of the data, yet preserving statistical fluctuations, we multiply each data point by the ratio of the unsmearred to smeared ansatz for each bin. This ratio ranges from 0.65 to 0.77, varying smoothly in  $P_T$ . Figure 2 shows the result of fitting equation 8 to the data for the smeared ansatz of equation 6. In addition, the corresponding unsmearred ansatz is shown. The corresponding plot of the smeared ansatz of equation 7 is indistinguishable on a log plot.

Figure 3 shows the residuals of the fit to smeared ansatz of equation 6. The fit yields a  $\chi^2/\text{dof} = 18.45/14$ . Neglecting inter-parameter correlations, we quote values  $N_1 = 7.94 \pm 0.42$ ,  $k_1 = 15.96 \pm 1.44$ ,  $N_2 = 3.56 \pm 0.67$  and  $k_2 = 33.98 \pm 3.21$ . There does not appear to be any systematic trend to the residuals. Repeating the process for the smeared ansatz of equation 7 yields similar results ( $\chi^2/\text{dof} = 17.33/15$ ). This fit yields  $N = (9.56 \pm 0.17) \times 10^7$ ,  $\alpha = 3.195 \pm 0.004$  and  $\beta = 56.1 \pm 0.4$ . Realizing that the two different ansatzes might result in different correction factors, we investigated the variation in correction factors for the two functional forms. We found that for  $P_T > 100$  GeV, the variation is less than 5%.

## G. Extracting the Heavy Flavor Component

As the long-term goal is to determine the  $\mu$ -tagged jets from heavy flavor (and later exclusively from  $b$ -quark containing hadrons), one must first remove the contribution from light meson decay. While the fraction of  $b$  and  $c$  quark decay into muons is well known (1/9), the fraction of pions and kaons decaying into muons depends on the detector geometry. A detector of larger radius will have a larger contribution of muons from light meson decay. The  $c\tau$  for pions and kaons is 7.8 m and 3.7 m respectively. The inner radius the DØ solenoid is 0.52 m. However, hadrons can pass a considerable distance into the magnet and calorimeter without undergoing hadronic shower, substantially increasing the effective decay radius allowed. In addition, at high jet  $P_T$  it is possible that pion secondaries from hadron showers can penetrate an additional distance and also undergo decay into muons. Using Pythia [5] and a GEANT-based full DØ detector simulation, we can determine the fraction of  $\mu$ -tagged jets that are from heavy flavor. Figure 4 shows the fraction of  $\mu$ -tagged jets that come from jets which contain at least one  $b$  or  $c$ -quark

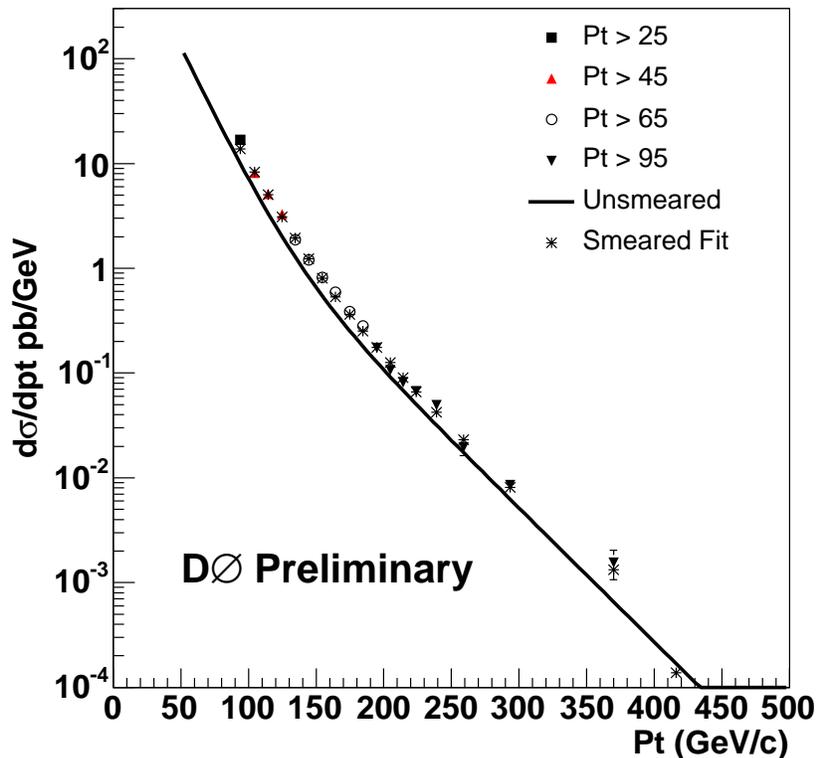


FIG. 2: Cross section for each trigger, corrected for efficiencies only. The solid line is the best-fit ansatz prior to smearing, while the asterisk is the best-fit of the ansatz after smearing due to jet resolution. In the legend, the  $P_T$  threshold for the Level 3 trigger is listed.

containing hadron. The overlaid fit is a functional form  $y = Ne^{-P_T/k} + O$ . The fit quality is reflected in the low  $\chi^2$  ( $\chi^2/\text{dof} = 25.4/23$ ) and yields parameters:  $N = 0.42 \pm 0.12$ ,  $k = 114 \pm 68$  and  $O = 0.44 \pm 0.06$ . The fraction ranges from about 70% at  $P_T = 50$  GeV, falling to about 45% at  $P_T = 400$  GeV. The dashed lines are a generous estimate of the systematic uncertainty, corresponding to  $\pm 20\%$ , and account for the uncertainty in the appropriate functional form. The large error bars simply reflect limited Monte Carlo statistics, thus this uncertainty (which is non-negligible at low jet  $P_T$ ) can be reduced.

#### H. Systematic Uncertainty

The final phase of the analysis is an estimate of the systematic uncertainty of the measurement. The relevant  $P_T$ -independent uncertainties are: overall efficiency uncertainty 13%, ansatz functional-form 5%, luminosity 6.5% and heavy-flavor fraction 20%. The  $P_T$  dependent uncertainty comes from the jet energy scale [4]. To estimate this uncertainty, the jet energy scale was increased/decreased by one standard deviation for each event and the analysis repeated. The ratio of these cross sections to the nominal cross section determined the contribution to the systematic uncertainty from the jet energy scale. This uncertainty was  $\pm 20\%$  at  $P_T = 100$  GeV and rises to  $+80\% / -50\%$  at  $P_T = 400$  GeV. The functional forms of the error band (in the region of validity  $100 < P_T < 400$  GeV) are:  $y = 123.4 - 0.1524P_T + 7.19 \times 10^{-4}P_T^2$  ( $+1\sigma$ ) and  $y = 89.33 - 3.43 \times 10^{-3}P_T - 2.00 \times 10^{-4}P_T^2$  ( $-1\sigma$ ).

### III. COMPARISON TO THEORY

As a final addition to the analysis, we compare the data with simple theory calculations. The first calculation was determined by simply running Pythia [5] and running an equivalent jet algorithm at the particle level. However,

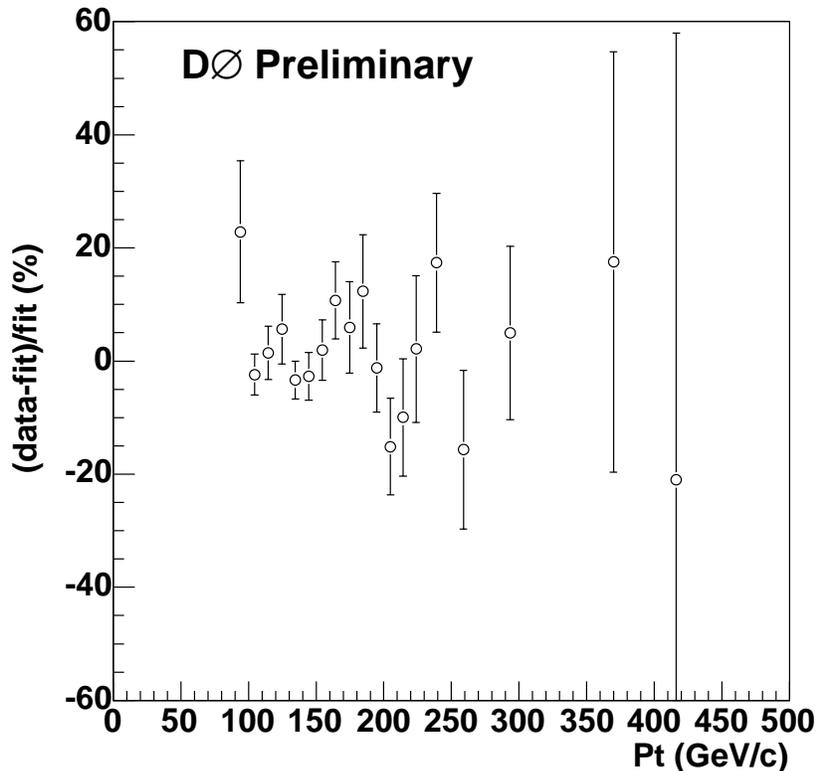


FIG. 3: Percentage residuals of the data as compared to the smeared ansatz.

since Pythia reflects only a leading order approximation to the cross section, we attempt to determine a  $k$ -factor so as to compare to next-to-leading order (NLO) theory. NLOJET++ [6] is a NLO calculation. However to adapt this calculation to  $\mu$ -tagged jets, we first run Pythia and determine a  $P_T$ -dependent fraction of jets that are  $\mu$ -tagged. We multiply this fraction to the cross section determined using NLOJET++ (CTEQ6M,  $\mu = P_T/2$ ) so as to estimate NLO  $\mu$ -tagged jet calculation.

Figure 5 shows a comparison between this measurement and both Pythia and our NLO estimate. The data sits approximately between the two calculations, with errors that nearly span the difference.

#### IV. SUMMARY

In this analysis, we present a measurement of the  $\mu$ -tagged jets coming from the decays of hadrons containing  $b$  and  $c$  quarks. The analysis is restricted to the central rapidity region  $|y| < 0.5$ . The integrated luminosity of the analysis includes  $294 \text{ pb}^{-1}$  of data. The data disagrees by about one standard deviation from both Pythia and a simple NLO calculation. A comparison to various quark-compositeness models will require a reduction in the jet energy scale uncertainty.

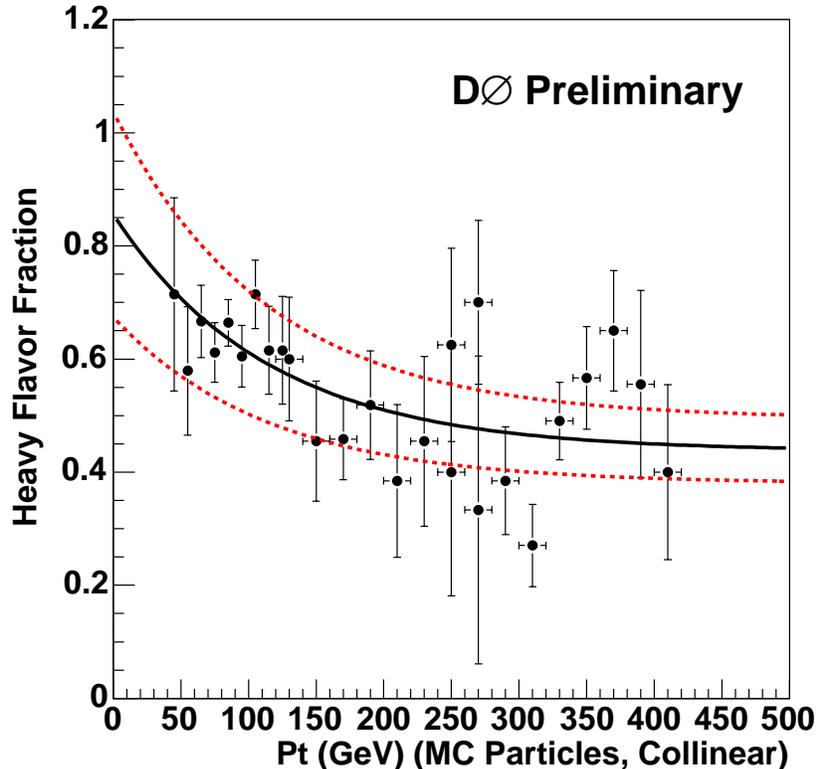


FIG. 4: Fraction of  $\mu$ -tagged jets coming from heavy-flavor content. The solid line denotes the fit described in the text, while the dashed lines are an estimate of the systematic uncertainty, including the uncertainty of the functional form of the fit.

#### Acknowledgments

We thank the staffs at Fermilab and collaborating institutions, and acknowledge support from the Department of Energy and National Science Foundation (USA), Commissariat à l’Energie Atomique and CNRS/Institut National de Physique Nucléaire et de Physique des Particules (France), Ministry of Education and Science, Agency for Atomic Energy and RF President Grants Program (Russia), CAPES, CNPq, FAPERJ, FAPESP and FUNDUNESP (Brazil), Departments of Atomic Energy and Science and Technology (India), Colciencias (Colombia), CONACyT (Mexico), KRF (Korea), CONICET and UBACyT (Argentina), The Foundation for Fundamental Research on Matter (The Netherlands), PPARC (United Kingdom), Ministry of Education (Czech Republic), Canada Research Chairs Program, CFI, Natural Sciences and Engineering Research Council and WestGrid Project (Canada), BMBF and DFG (Germany), Science Foundation Ireland, A.P. Sloan Foundation, Research Corporation, Texas Advanced Research Program, Alexander von Humboldt Foundation, and the Marie Curie Fellowships.

- 
- [1] DØ Collaboration, “The DØ Detector” (in preparation) (2005).  
[2] G.C Blazey *et al.*, in *Proceedings of the Workshop “QCD and Weak Boson Physics in Run II,”* edited by U. Baur, R. K. Ellis and D. Zeppenfeld, Batavia, Illinois (2000) p. 47. See Section 3.5 for Details.  
[3] C. Clement *et al.*, “MuonID Certification for p14”. DØNote 4350.  
[4] J.L Agram *et al.*, “Jet Energy Scale at DØ Run II”, DØNote 4720.  
[5] T. Sjöstrand *et al.*, *Comp. Phys. Comm.* **135**, 238 (2001).  
[6] Z. Nagy, *Phys. Rev. Lett.* **88**, 122003 (2002); Z. Nagy, *Phys. Rev. D* **68**, 094002 (2003).

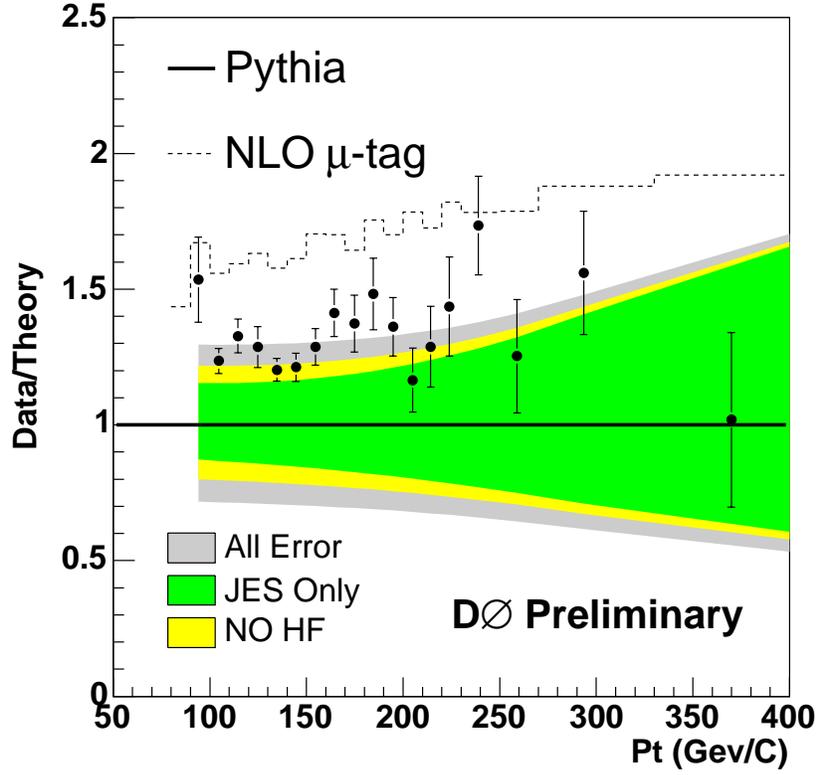


FIG. 5: Comparison of data to PYTHIA. Dashed line is the ratio of the NLO estimate to PYTHIA. The NLO estimate is simply NLOJET++ multiplied by PYTHIA's prediction of the fraction of all jets that are  $\mu$ -tagged. The outer error band denotes the full systematic uncertainty estimate for this analysis. The middle error band reduces the heavy-flavor fraction error to zero, while maintaining other errors at nominal. The inner error band denotes the contribution to the systematic uncertainty exclusively from the jet energy scale. These systematic error bands are a multiplicative factor and can be associated to either the data/PYTHIA or NLO/PYTHIA ratio.